The Mechanism of High Strength-Ductility Steel Produced by a Novel Quenching-Partitioning-Tempering Process and the Mechanical Stability of Retained Austenite at Elevated Temperatures

S. ZHOU, K. ZHANG, Y. WANG, J.F. GU, and Y.H. RONG

The designed steel of Fe-0.25C-1.5Mn-1.2Si-1.5Ni-0.05Nb (wt pct) treated by a novel quenching-partitioning-tempering (Q-P-T) process demonstrates an excellent product of strength and elongation (PSE) at deformed temperatures from 298 K to 573 K (25 °C to 300 °C) and shows a maximum value of PSE (over 27,000 MPa pct) at 473 K (200 °C). The results fitted by the exponent decay law indicate that the retained austenite fraction with strain at a deformed temperature of 473 K (200 °C) decreases slower than that at 298 K (25 °C); namely, the transformation induced plasticity (TRIP) effect occurs in a larger strain range at 473 K (200 °C) than at 298 K (25 °C), showing better mechanical stability. The work-hardening exponent curves of Q-P-T steel further indicate that the largest plateau before necking appears at the deformed temperature of 473 K (200 °C), showing the maximum TRIP effect, which is due to the mechanical stability of considerable retained austenite. The microstructural characterization reveals that the high strength of Q-P-T steels results from dislocation-type martensite laths and dispersively distributed fcc NbC or hcp ε-carbides in martensite matrix, while excellent ductility is attributed to the TRIP effect produced by considerable retained austenite.

DOI: 10.1007/s11661-011-0929-z

I. INTRODUCTION

ADVANCED high-strength steels (AHSS) containing substantial amounts of retained austenite have been the subject of many recent investigations due to their good combination of strength and ductility.[1–4] Recently, Hsu[5] proposed a novel quenching-partitioning-tempering (Q-P-T) process, with the microstructure of Q-P-T steels consisting of lath martensite, fine complex alloying carbides, and flakelike carbon-enriched retained austenite. Similar to quenching and partitioning (Q&P) technology previously proposed by Speer *et al.*,[3,6] the Q-P-T process includes a quenching treatment from the austenite state to a quenching temperature (T_Q) between the start temperature of martensitic transformation (M_s) and the final temperature (M_f). Then, an isothermal holding (partitioning/tempering) treatment is operated, during which carbon diffuses from the supersaturated martensite into the neighboring untransformed austenite, thereby stabilizing retained austenite during sequent cooling to room temperature; meanwhile, stable alloying carbides (such as NbC) precipitate from the martensite matrix and provide the potential of precipitation strengthening, which was excluded in the Q&P process for satisfying the "Constrained Carbon Paraequilibrium" theory proposed by Speer *et al.*[3,6] Our previous research[7,8] on cold-rolled sheets showed that steels subjected to Q-P-T processes exhibited an excellent combination of strength and ductility.

Great efforts were made for understanding the relationship between the microstructure and the mechanical property of Q-P-T steels. However, the mechanism of high strength-ductility of Q-P-T steels and the stability of retained austenite at elevated temperatures were not investigated. Therefore, the aim of the present article is to study the mechanical properties of the Q-P-T steel designed at elevated temperatures and the stability of the retained austenite so as to reveal the mechanism of high strength-ductility and to evaluate the temperature range to which the Q-P-T steel studied can be subjected.

II. EXPERIMENTAL PROCEDURE

The chemical compositions of the Q-P-T steel investigated are listed in Table I, together with Ac_3, M_s, and M_f temperatures, which were determined by a Gleeble-3500 thermal simulator (Gleeble, Dynamic Systems Inc. (DSI), Poestenkill, NY). Addition of Si element is to suppress the formation of cementite (Fe_3C). Elements Mn and Ni are used to stabilize austenite and lower M_s temperature. Element Nb can effectively not only refine original austenite grains but also stabilize carbide formation, which leads to grain-refinement strengthening and precipitation strengthening. Experimental samples with a dimension of $105 \times 22 \times 2.5$ mm^3 were cut, parallel to the rolling

S. ZHOU, K. ZHANG, and Y. WANG, Doctoral Students, and J.F. GU and Y.H. RONG, Professors, are with the School of Materials Science and Engineering, Shanghai Jiao Tong University, Shanghai 200240, P.R. China. Contact e-mail: yhrong@sjtu.edu.cn
Manuscript submitted June 8, 2011.
Article published online October 19, 2011

direction, from a 20-mm-thick hot-rolled plate supplied by the Technical R&D Center of Laiwu Steel Group (Shangdong, P.R. China). For the Q-P-T process, samples were austenitized at 1203 K (930 °C) for 600 seconds, followed by quenching into a molten salt bath at 563 K (290 °C) for 15 seconds. Subsequently, they were tempered at 698 K (425 °C) in a second salt bath for 30 seconds, and finally water quenched to room temperature.

The as-treated samples were then machined into plate tensile specimens with 6-mm width, 2-mm thickness, and 20-mm length. Tensile tests were carried out in the temperature range from 298 K to 673 K (25 °C to 400 °C) using a SANS 5105 testing machine (MTS Systems Corporation, Shanghai, P.R. China) fitted with a 100 kN load cell. An extension rate of 0.5 mm/min was used in all tensile experiments. Before tensile tests, all the specimens were isothermally held at each target temperature for 600 seconds so that the entire specimen could be uniformly heated. Moreover, two specimens for each process were subjected to tensile tests and an average value of mechanical properties was calculated. If the test values of these two specimens for a given process have a large difference (above 10 pct), a third one will be tested.

The work-hardening coefficient (n) was calculated using the classical Hollomon equation:[9]

$$\sigma = K\varepsilon^n \qquad [1]$$

where σ is true stress, ε is true strain, K is a constant, and n is the incremental work hardening exponent. Then, n can be written as

$$n = \frac{\varepsilon}{\sigma}\frac{d\sigma}{d\varepsilon} \qquad [2]$$

when $\frac{d\sigma}{d\varepsilon} = \sigma$ (necking criterion), and then

$$n = \varepsilon_u \qquad [3]$$

where ε_u is the maximum value of uniform elongation.

Volume fraction of retained austenite in the undeformed samples after isothermal holding for 600 seconds at elevated temperatures was quantified by X-ray diffraction (XRD) with Cu K_α radiation using a D/max 2550 X-ray diffraction analyzer (Rigaku Corporation, Tokyo, Japan) at 35 kV and 200 mA. The 2θ angular interval from 35 to 105 deg was step-scanned with a scanning speed (2θ) of 5 deg/min. Retained austenite composition was calculated using the direct comparison method[10] from the integrated intensities of (200), (220), and (311) austenite peaks and those of (200) and (211) martensite peaks. Furthermore, the variation of retained austenite contents with strain during tensile tests at 298 K and 473 K (25 °C and 400 °C), respectively, has also been measured.

Microstructure characterization was performed in a FEI SIRION 200 scanning electron microscope (SEM, FEI Company, Hillsboro, OR) and JEM 2100F transformation electron microscope (TEM, JEOL Company, Tokyo, Japan). The samples for SEM were polished and etched in 2 pct nital solution. Selected samples for TEM were prepared by slicing into 3-mm-o.d. discs and grinding from 300-μm to 40-μm-thick foils. Subsequently, these foils were electropolished at 253 K (–20 °C) in an MTP-1A twin-jet polisher using the electrolyte consisting of 4 pct perchloric

Table I. Chemical Compositions and Characteristic Temperatures of the Experimental Q-P-T Steel (Weight Percent)

C	Si	Mn	Ni	Nb	P	S	Ac_3 (K)	M_s (K)	M_f (K)
0.256	1.2	1.48	1.51	0.053	0.017	0.008	1153 ± 5	678 ± 5	483 ± 3

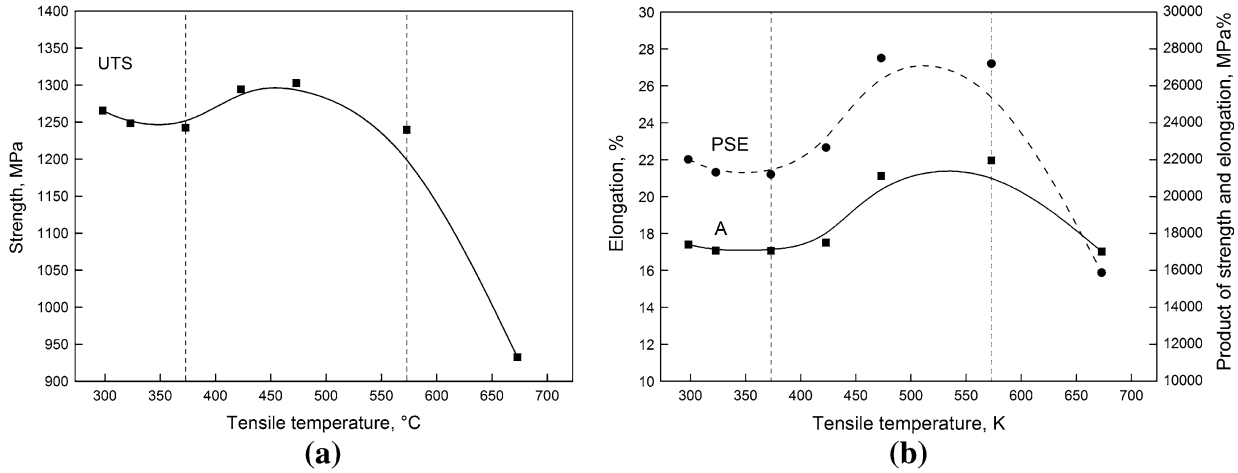

Fig. 1—Mechanical properties of Q-P-T steels as functions of tensile temperature: (*a*) strength and (*b*) elongation and strength-elongation product.

acid and 96 pct ethanol solution. TEM examination was carried out at an operating voltage of 200 kV using a bright-field (BF) image, dark-field (DF) image, and selected area electron diffraction (SAED) mode.

III. RESULTS AND DISCUSSION

A. *Dependence of Mechanical Properties on Temperature*

As shown in Figure 1, ultimate tensile strength (UTS), total elongation (A), and product of strength and elongation (PSE) from tensile tests, as functions of tensile temperature, all exhibit a three-stage variation as follows. (1) Temperature regime I between 298 K and 373 K (25 °C and 100 °C); values of UTS, A, and PSE almost remain constant, while the yield strength decreases slightly from 1067 to 1022 MPa, showing the most stable stage of Q-P-T steel. (2) Temperature regime II from 373 K to 573 K (100 °C to 300 °C); values of UTS, A, and PSE exhibit the same tendency, including a slow increase in the beginning and a slight drop afterward as tensile temperature rises. When tensile specimens are deformed at 473 K (200 °C), PSE exhibits a superior high value of over 27,000 MPa pct, which is much higher than the 25,000 MPa pct that AHSS usually reaches. (3) Temperature regime III above 573 K (300 °C); the mechanical properties of the as-treated samples significantly deteriorate with increasing tensile temperature.

B. *Evolution of Retained Austenite Fraction with Different Tensile Temperatures*

In the present work, the volume fraction of retained austenite is determined by quantitative analysis of XRD data. Figure 2 presents the variation of retained austenite fractions in the undeformed samples after isothermal holding for 600 seconds at each deformed temperature from 298 K to 673 K (25 °C to 400 °C). It is clear that retained austenite exhibits good thermal stability from 298 K to 573 K (25 °C to 300 °C); that is, retained austenite remains nearly unchanged at 12 pct at the first stage [temperature regime I, 298 K (25 °C) ≤ T ≤ 373 K (100 °C)], and retained austenite decreases slightly from 12 to 9.5 pct at the second stage [temperature regime II, 373 K (100 °C) ≤ T ≤ 573 (300 °C)]. However, at the third stage [temperature regime III, 573 (300 °C) ≤ T ≤ 673 K (400 °C)], the amount of retained austenite quickly drops to below 5 pct, implying the decomposition of retained austenite. Although the addition of Si can suppress the decomposition of original austenite to ferrite and cementite at relative high temperatures, the retained austenite in the steels treated by the Q-P-T process is carbon-enriched, and the amount of Si in retained austenite would be very small due to the positive activity coefficient of C to Si. Therefore, the decomposition of the retained austenite with little Si in Q-P-T steels will occur during tensile tests in temperature regime III.

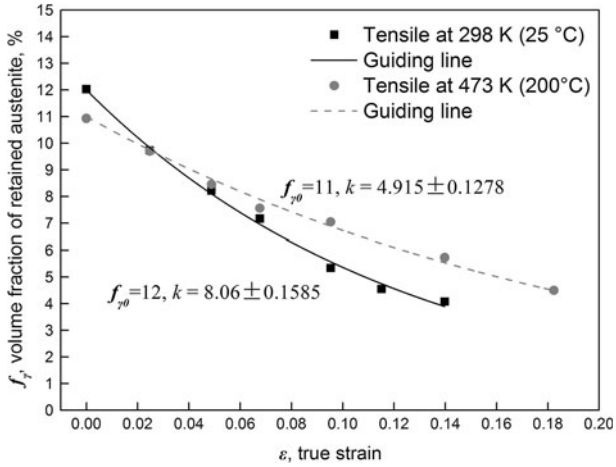

Fig. 3—Austenite fraction as a function of true tensile strain during plastic deformation at 298 K and 473 K (25 °C and 200 °C).

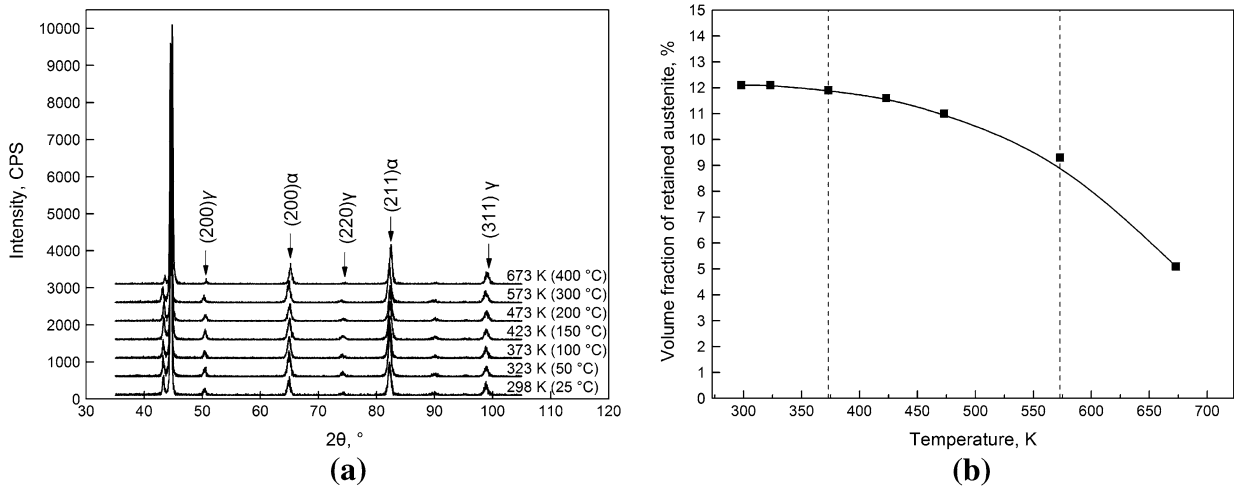

Fig. 2—Initial retained austenite fractions of the undeformed tensile samples as a function of deformed temperature: (*a*) Diffraction spectra of the samples and (*b*) evolution of the retained austenite fraction *vs* deformed temperature.

The evolution of retained austenite fraction during plastic deformation at 298 K and 473 K (25 °C and 200 °C) is presented in Figure 3. It can be seen that both curves decrease monotonically with true strain, which can be fitted well by the exponent decay law proposed by Sugimoto *et al.*[11] and Sherif *et al.*[12] as follows:

$$f_\gamma = f_{\gamma 0} \exp(-k\varepsilon) \quad [4]$$

where f_γ is the austenite fraction at strain ε; $f_{\gamma 0}$ is the initial austenite fraction before tensile tests at each temperature obtained from Figure 2(b); and k is a constant, representing the mechanical stability of retained austenite associated with the driving force for the transformation of retained austenite to martensite.

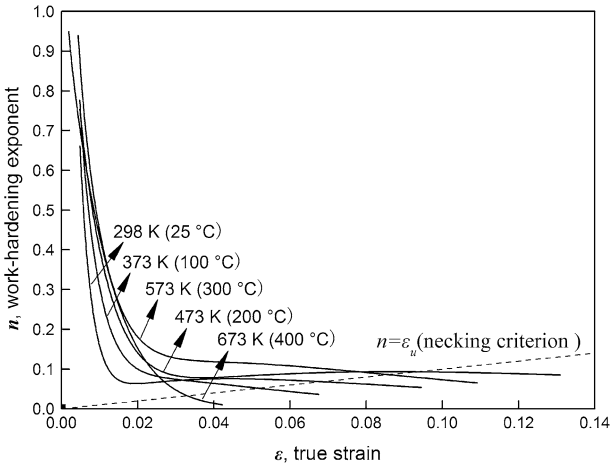

Fig. 4—Work-hardening behaviors of Q-P-T samples during plastic deformation at different tensile temperatures.

Based on the preceding formula, we can see that tensile specimens with a smaller k may reach a larger strain ε when $f_\gamma/f_{\gamma 0}$ remains constant. Moreover, comparing these two curves in Figure 3, although the amount of initial retained austenite ($f_{\gamma 0}$) at 473 K (200 °C) is a little lower than that at 298 K (25 °C), it decreases with a slower decreasing rate accompanied with a relatively large strain during plastic deformation, showing its better mechanical stability. Therefore, it can be concluded that high temperature effectively decreases the driving force of the transformation of austenite to martensite. Thus, martensitic transformation needs large strain to generate, which leads to the existence of more retained austenite at 473 K (200 °C) than at 298 K (25 °C) for the same strain level; namely, the transformation-induced plasticity (TRIP) effect occurs in a larger strain range (over 18 pct) at 473 K (200 °C) than 14 pct at 298 K (25 °C).

C. *Work-Hardening Behaviors*

As is known, the instantaneous work-hardening exponent curve of TRIP steel containing an adequate amount of metastable austenite exhibits three stages: a first stage with the work-hardening exponent decreasing rapidly in the normal way, a second stage with a plateau before necking, and a third stage with a second slow decrease.[13–16] The second stage with a plateau is considered to be associated with the mechanical stability of retained austenite and the TRIP effect produced by the transformation of retained austenite to martensite, which enhance the elongation of TRIP steel. The third stage shows a weak effect of retained austenite and a tendency of tensile specimens to fracture. Similarly, the as-treated Q-P-T steel in the present work exhibits the

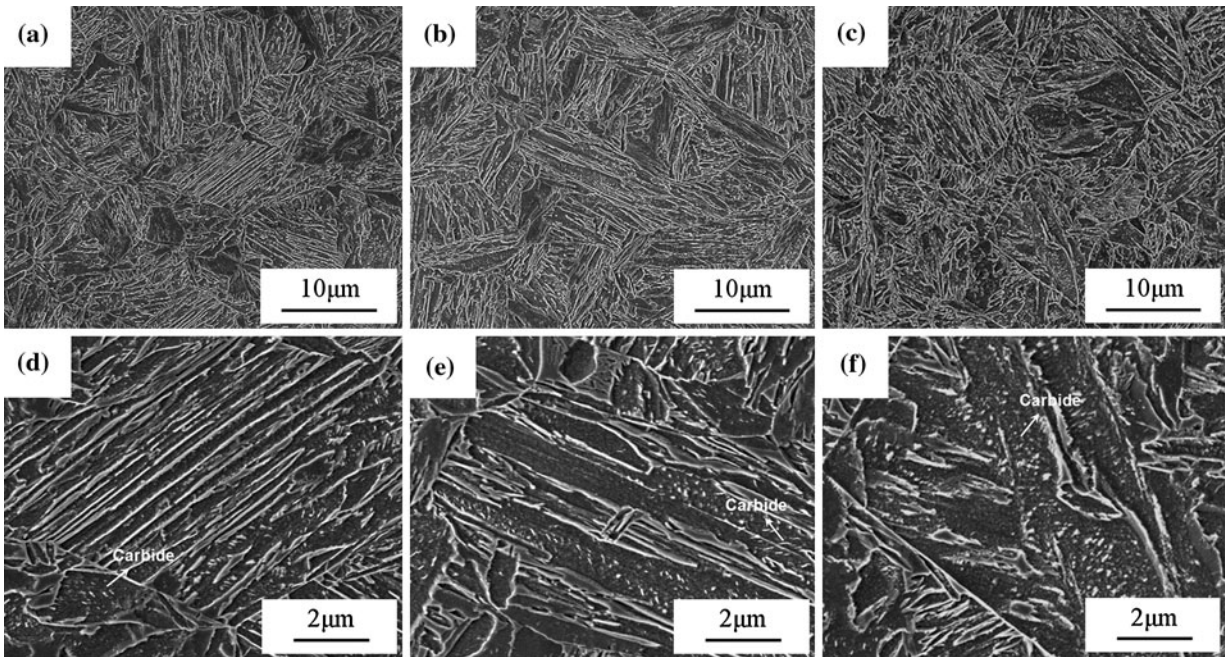

Fig. 5—SEM micrographs of the undeformed experimental samples at (*a*) 298 K (25 °C), (*b*) 473 K (200 °C), and (*c*) 673 K (400 °C) and (*d*), (*e*), and (*f*) corresponding magnified micrographs.

same work-hardening behaviors during plastic deformation below 573 K (300 °C), as shown in Figure 4. Plateaus in stage II can be observed before necking ($n = \varepsilon_u$) at various deformed temperatures. The widest two plateaus are at 473 K and 573 K (200 °C and 300 °C), showing the maximum TRIP effect of retained austenite on the improvement of strength and elongation, which is consistent with the values of PSE in Figure 1(b). Nevertheless, the instantaneous work-hardening exponent (n) of the samples deformed at 673 K (400 °C) decreases rapidly with true strain (ε), and no plateau exists during the entire plastic deformation, which agrees with the weak TRIP effect due to the low amount of retained austenite.

D. *Microstructural Characterization*

SEM micrographs of the undeformed samples at 298 K, 573 K, and 673 K (25 °C, 200 °C, and 400 °C) are shown in Figure 5, respectively. It is clear that the microstructures of these three undeformed Q-P-T samples are typical lath martensite. However, the long and straight feature of martensite laths in magnified micrographs becomes weak gradually with the increase of temperature. Moreover, retained austenite cannot be distinguished from martensite laths in Figure 5, but fine carbides can be gradually observed with the increase of temperature.

In order to further identify the microstructures, TEM observation were performed on three typical Q-P-T specimens before and after tensile tests at 298 K, 473 K, and 673 K (25 °C, 200 °C, and 400 °C). Figure 6 shows the microstructural features of the undeformed Q-P-T samples before tensile tests at 298 K and 473 K (25 °C and 200 °C). It can be seen that the multiphase microstructure in the samples comprises dislocation-type lath martensite and flakelike retained austenite between martensite laths. The orientation relationships between martensite matrix and retained austenite are identified by the inserted SAED pattern in Figure 6(b) as the Kurdjumov-Saches (K-S)

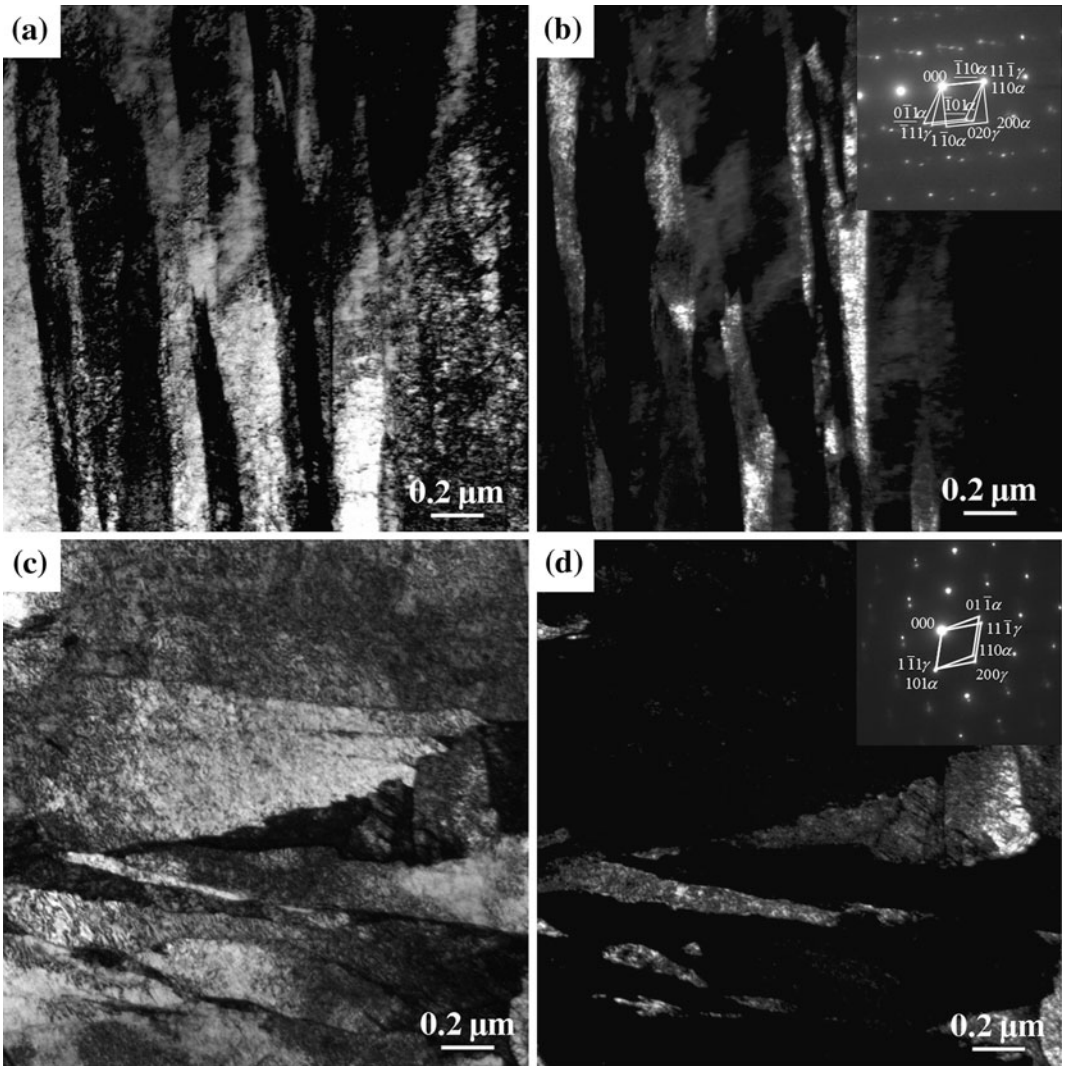

Fig. 6—TEM micrographs of the undeformed Q-P-T specimens at 298 K and 473 K (25 °C and 200 °C): (*a*) 298 K (25 °C), BF image; (*b*) 298 K (25 °C), DF image of retained austenite and inserted SAED; (*c*) 473 K (200 °C), BF image; and (*d*) 473 K (200 °C), DF image of retained austenite and inserted SAED.

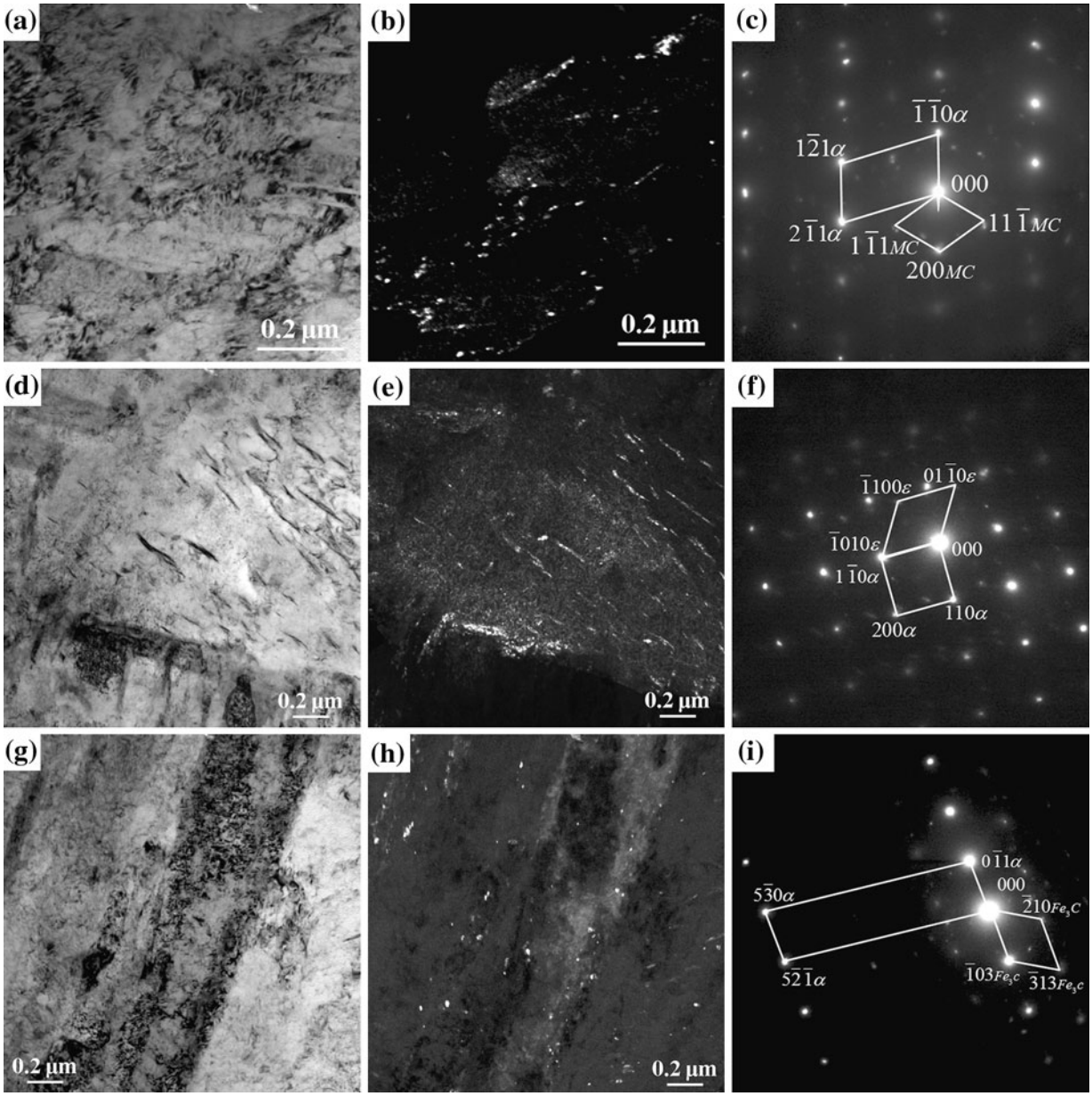

Fig. 7—TEM micrographs show carbides in the undeformed Q-P-T sample at 298 K, 473 K, and 673 K (25 °C, 200 °C, and 400 °C): (*a*) 298 K (25 °C), BF image; (*b*) 298 K (25 °C), DF image of carbides; (*c*) SAED pattern; (*d*) 473 K (200 °C), BF image; (*e*) 473 K (200 °C), DF image of carbides; (*f*) SAED pattern; (*g*) 673 K (400 °C), BF image; (*h*) 673 K (400 °C), DF image of carbides; and (*i*) SAED pattern.

relationship: $[111]\alpha // [101]\gamma$, $(\bar{1}10)\alpha // (11\bar{1})\gamma$, and the Nishiyama-Wassermann (N-W) relationship: $[001]\alpha // [101]\gamma$, $(110)\alpha // (11\bar{1})\gamma$; and in Figure 6(d) as the K-S relationship: $[\bar{1}11]\alpha // [011]\gamma$, $(101)\alpha // (1\bar{1}1)\gamma$. Nevertheless, the amount of flakelike retained austenite in undeformed samples at 473 K (200 °C) is slightly less than that at 298 K (25 °C). Moreover, flakelike retained austenite was not observed in the undeformed specimen at 673 K (400 °C) by TEM due to its very low amount, which is also consistent with the XRD results in Figure 2(b).

Figure 7 presents fine precipitated complex carbides dispersed in the undeformed Q-P-T samples at 298 K, 473 K, and 673 K (25 °C, 200 °C and 400 °C). From Figures 7(a) and (b), it can be seen that large numbers of spherical carbides with an average size of 20 ± 5 nm precipitate in the martensite matrix. Based on our previous research[17] and the SAED pattern (Figure 7(c)), it can be concluded that these fine alloying carbides are Nb-containing complex alloying ones and can provide a significant precipitation strengthening effect in Q-P-T steels. The orientation relationship between the martensite matrix and these Nb-containing carbides is identified as $[113]\alpha // [011]_{MC}$ and $(\bar{1}\bar{1}0)\alpha // (100)_{MC}$. It is interesting that, besides these spherical Nb-containing carbides, the majority of carbides in the undeformed Q-P-T samples at 473 K (200 °C) exhibit in sheet shape, as shown in Figures 7(d) and (e). These carbides are identified as transitional hcp ε-carbides by the SAED pattern (Figure 7(f)). The orientation relationship between the martensite matrix and ε-carbides is

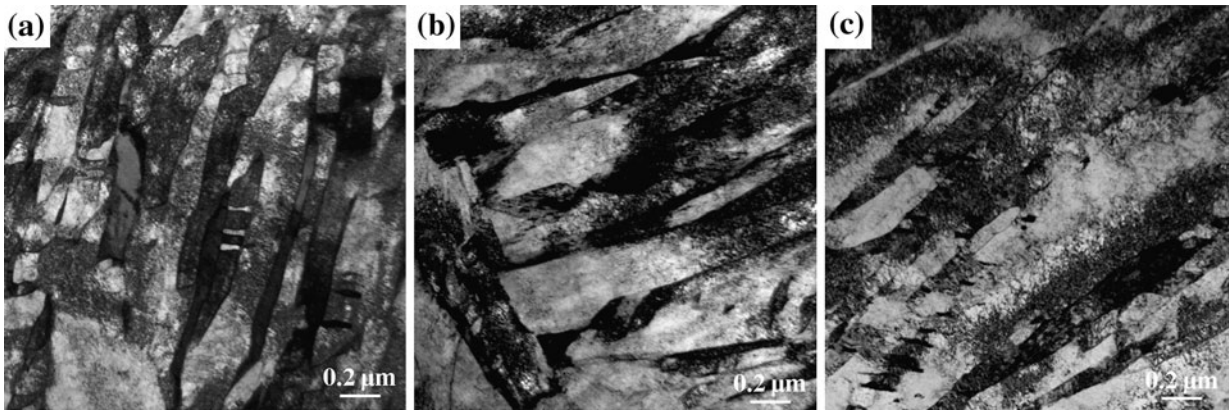

Fig. 8—TEM BF images of the microstructures near the tensile fracture on the Q-P-T samples at 298 K, 473 K, and 673 K (25 °C, 200 °C, and 400 °C): (*a*) 298 K (25 °C), (*b*) 473 K (200 °C), and (*c*) 673 K (400 °C).

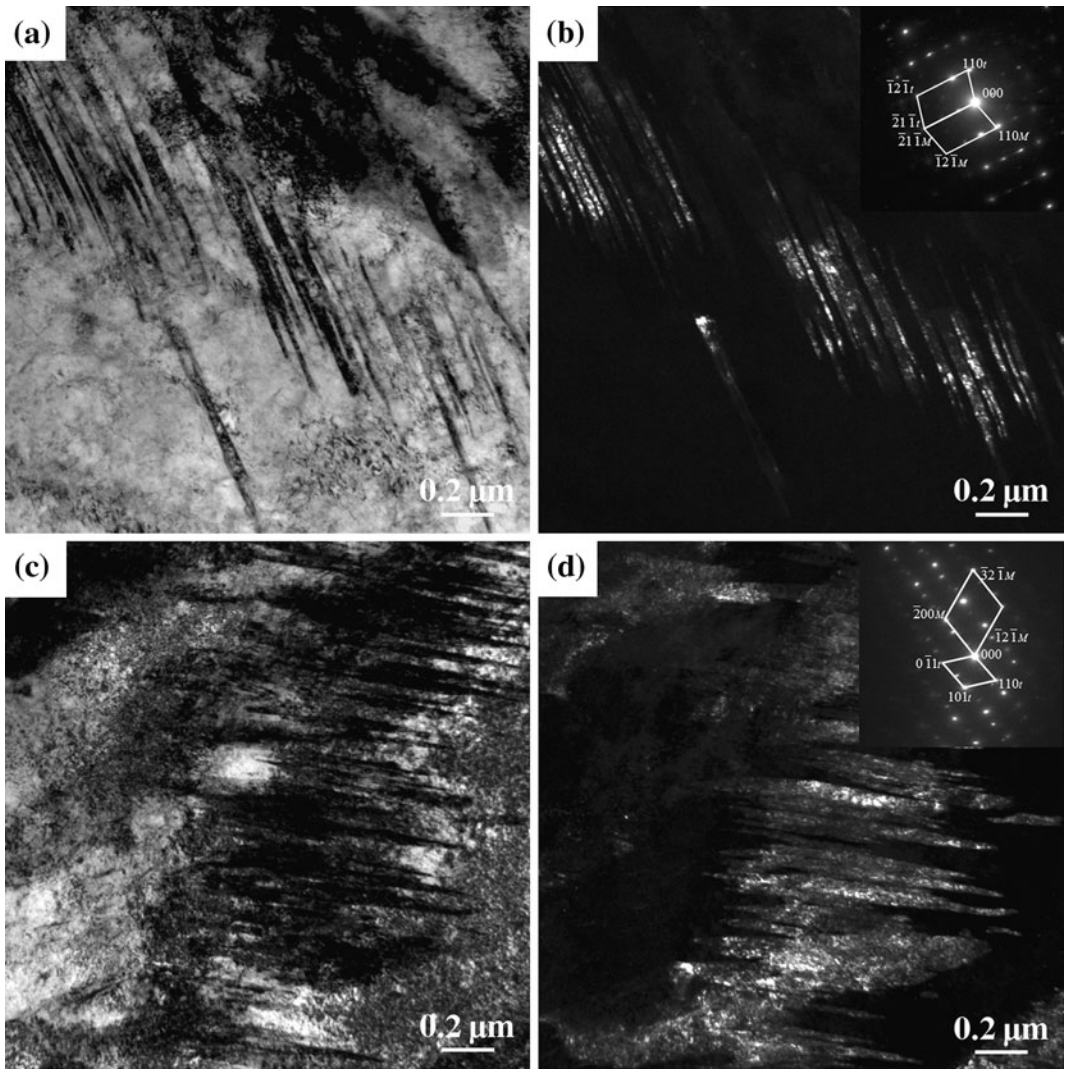

Fig. 9—TEM micrographs of twin-type martensite near the tensile fracture on the Q-P-T samples at 298 K and 473 K (25 °C and 200 °C): (*a*) 298 K (25 °C), BF image; (*b*) 298 K (25 °C), DF image of twin-type martensite and inserted SAED pattern; (*c*) 473 K (200 °C), BF image; and (*d*) 473 K (200 °C), DF image of twin-type martensite and inserted SAED pattern.

$[001]\alpha//[0001]\varepsilon$, $(1\bar{1}0)\alpha//(\bar{1}010)\varepsilon$. These ε-carbides were reported as a metastable phase formed in martensitic steels with 0.1 to 0.5 wt pct carbon during tempering at relatively low temperatures [373 K to 573 K (100 °C to 300 °C)], and may transform to cementite, which is thought to be harmful to the toughness and ductility of steels after tempering at a higher temperature.[18–21] Furthermore, it should be pointed out that, since these ε-carbides have not transformed to cementite, Q-P-T tensile specimens present the best combination of strength and ductility during plastic deformation at 473 K (200 °C). Also, the reasonable explanation for the enhancement of both strength and elongation in Q-P-T steels at 473 K (200 °C) can be described as follows. It can be seen from Figure 2 that the volume fraction of retained austenite in undeformed samples changed slightly in temperature regimes I and II; thus, the amount of stress-induced martensite from retained austenite during tensile tests is hardly reduced and contributes to the strength of steels. For example, the decrement of retained austenite during tensile tests at 298 K (25 °C) is calculated to be close to that at 473 K (200 °C), as shown in Figure 3. Therefore, both the enough stress-induced martensite and the large amount of ε-carbides precipitated from the martensite matrix compensate the softening of microstructure during tensile tests at 473 K (200 °C). The carbides in undeformed Q-P-T samples at 673 K (400 °C) are shown in Figures 7(g) and (h). It can be seen that most transitional ε-carbides disappear after isothermal holding at the relatively high temperature. These carbides in Figures 7(g) and (h) also appear in spherical shape with an average grain size of 20 ± 5 nm, but are identified as cementite by the SAED pattern (Figure 7(i)). As mentioned previously, Q-P-T tensile specimens presented the worst mechanical performance during plastic deformation at 673 K (400 °C). This finding can be well explained as follows. Figure 2 shows that the amount of undeformed retained austenite sharply decreases to lower than 5 pct before tensile tests at 673 K (400 °C); as a result, the TRIP effect from retained austenite during tensile tests is so weak that its contribution to the strength and elongation of Q-P-T steels can be almost neglected. Moreover, the precipitation of cementite in the martensite matrix in Figures 7(g) and (h) may further harm the ductility of Q-P-T steels. In general, the weak TRIP effect and the precipitation of cementite, together with the softening of microstructure, lead to the poor mechanical properties of Q-P-T specimens during tensile tests at 673 K (400 °C). Moreover, TEM observation also indicates that the addition of alloying element Si in Q-P-T steels can only delay the precipitation of Fe_3C in martensite matrix at relatively low temperatures, but cannot suppress the formation of Fe_3C at relatively high temperatures.

The microstructures near the tensile fracture of the deformed samples at 298 K, 473 K, and 673 K (25 °C, 200 °C, and 400 °C) were also investigated by TEM, respectively, as shown in Figure 8. It can be seen that the main features of these deformed samples are the large numbers of dislocation tangles and subgrains formed in martensite laths. Besides, twin-type martensite sheets in the deformed samples at 298 K and 473 K (25 °C and 200 °C) are observed in Figure 9, which are formed during the transformation of carbon-enriched retained austenite to martensite, namely, the product of the TRIP effect. However, there is no remarkable twin-type martensite in the microstructure of the samples deformed at 673 K (400 °C) due to the weak TRIP effect of retained austenite.

IV. CONCLUSIONS

The mechanical properties of Q-P-T steels and the stability of retained austenite at different deformed temperatures were investigated by tensile tests, XRD, SEM, and TEM. The main conclusions are described as follows.

1. The results of tensile tests and XRD indicate that retained austenite exhibits good mechanical stability at deformed temperatures from 298 K to 573 K (25 °C to 300 °C); that is, the almost unchanged volume fraction of retained austenite in the first stage [298 K (25 °C) $\le T \le$ 373 K (100 °C)], a slight decrease of volume fraction of the retained austenite in the second stage [373 K (100 °C) $\le T \le$ 573 K (300 °C)], and a dramatic drop of the volume fraction of retained austenite in the third stage [573 K (300 °C) $\le T \le$ 673 K (400 °C)] are exhibited. Therefore, the Q-P-T steels studied in this work can be applied at the temperature range from 298 K to 573 K (25 °C to 300 °C).
2. Q-P-T steels possess a high PSE from 298 K to 573 K (25 °C to 300 °C), in which high strength results from dislocation-type martensite laths and dispersively distributed carbides in martensite matrix, while excellent ductility is attributed to considerable retained austenite and its TRIP effect. The mechanical properties of Q-P-T steels show a further increase during tensile tests at higher temperature [373 K (100 °C) $\le T \le$ 573 K (300 °C)] because of the precipitation of hcp ε-carbides and the better mechanical stability of considerable retained austenite with its volume fraction slightly changed. However, when deformed temperature is over 573 K (300 °C), PSE dramatically drops due to the sharply decreased volume fraction of retained austenite and the formation of cementite.
3. TEM observation indicates that the addition of Si to Q-P-T steels can suppress the formation of cementite in the martensite matrix at deformed temperatures from 298 K to 573 K (25 °C to 300 °C), but cannot prevent the precipitation of hcp ε-carbides during tensile tests at 373 K (100 °C) $\le T \le$ 573 K (300 °C) or the formation of cementite at temperatures above 573 K (300 °C).

ACKNOWLEDGMENT

This study was financially supported by the National Natural Science Foundation of China (Grant No. 51031001) and Laiwu Steel Group (Shandong, China).

REFERENCES

1. P.J. Jacques, E. Girault, A. Mertens, B. Verlinden, J. Van Humbeeck, and F. Delannay: *ISIJ Int*., 2001, vol. 41, pp. 1068–74.
2. F.G. Caballero and H.K.D.H. Bhadeshia: *Curr. Opin. Solid State Mater. Sci*., 2004, vol. 8, pp. 251–57.
3. J.G. Speer, D.V. Edmonds, F.C. Rizzo, and D.K. Matlock: *Curr. Opin. Solid State Mater. Sci*., 2004, vol. 8, pp. 219–37.
4. F.G. Caballero, M.J. Santofimia, C. García-Mateo, J. Chao, and C.G. de Andrés: *Mater. Des*., 2009, vol. 30, pp. 2077–83.
5. T.Y. Hsu: *Mater. Sci. Forum*, 2007, vols. 561–565, pp. 2283–86.
6. J.G. Speer, D.K. Matlock, B.C. De Cooman, and J.G. Schroth: *Acta Mater*., 2003, vol. 51, pp. 2611–22.
7. X.D. Wang, N. Zhong, Y.H. Rong, T.Y. Hsu, and L. Wang: *J. Mater. Res*., 2009, vol. 24, pp. 260–67.
8. N. Zhong, X.D. Wang, L. Wang, and Y.H. Rong: *Mater. Sci. Eng., A*, 2009, vol. 506, pp. 111–16.
9. W.C. Leslie: *The Physical Metallurgy of Steel*, McGraw-Hill Co, New York, NY, 1981, p. 1.
10. J. Durnin and K.A. Ridal: *J. Iron Steel Inst*., 1968, vol. 206, pp. 60–67.
11. K.I. Sugimoto, M. Kobayashi, and S.I. Hashimoto: *Metall. Trans. A*, 1992, vol. 23A, pp. 3085–91.
12. M.Y. Sherif, C.G. Mateo, T. Sourmail, and H.K.D.H. Bhadeshia: *Mater. Sci. Technol*., 2004, vol. 20, pp. 319–22.
13. D.B. Santos, R. Barbosa, P.P.d. Oliveira, and E.V. Pereloma: *ISIJ Int*., 2009, vol. 49, pp. 1592–1600.
14. I.B. Timokhina, P.D. Hodgson, and E.V. Pereloma: *Metall. Mater. Trans. A*, 2003, vol. 34A, pp. 1599–1609.
15. I.B. Timokhina, P.D. Hodgson, and E.V. Pereloma: *Metall. Mater. Trans. A*, 2004, vol. 35A, pp. 2331–41.
16. J. Shi, X. Sun, M. Wang, W. Hui, H. Dong, and W. Cao: *Scripta Mater*., 2010, vol. 63, pp. 815–18.
17. X.D. Wang, W.Z. Xu, Z.H. Guo, L. Wang, and Y.H. Rong: *Mater. Sci. Eng., A*, 2010, vol. 527, pp. 3373–78.
18. Y. Ohmori and I. Tamura: *Metall. Trans. A*, 1992, vol. 23A, pp. 2737–51.
19. Y. Tan: *Acta Metall. Sinica*, 1985, vol. 21, pp. 181–86.
20. D.V. Edmonds, K. He, M.K. Miller, F.C. Rizzo, A. Clarke, D.K. Matlock, and J.G. Speer: *5th Int. Conf. on Processing and Manufacturing of Advanced Materials*, Vancouver, Canada, 2006, pp. 4819–25.
21. H.Y. Li, X.W. Lu, W.J. Li, and X.J. Jin: *Metall. Mater. Trans. A*, 2010, vol. 41A, pp. 1–17.